



Enhanced thermoelectric properties of $\text{Cu}_2\text{ZnSnSe}_4$ with Ga-doping



Kaya Wei ^a, Laura Beauchemin ^a, Hsin Wang ^b, Wallace D. Porter ^b, Joshua Martin ^c,
George S. Nolas ^{a,*}

^a Department of Physics, University of South Florida, Tampa, FL 33620, USA

^b Materials Science and Technology Division, Oak Ridge National Laboratory, Oak Ridge, TN 37831, USA

^c Material Measurement Laboratory, National Institute of Standards and Technology, Gaithersburg, MD 20899, USA

ARTICLE INFO

Article history:

Received 21 June 2015

Accepted 6 August 2015

Available online 10 August 2015

Keywords:

Quaternary chalcogenides

Thermoelectric properties

Gallium doping

ABSTRACT

Gallium doped $\text{Cu}_2\text{ZnSnSe}_4$ quaternary chalcogenides with and without excess Cu were synthesized by elemental reaction and densified using hot pressing in order to investigate their high temperature transport properties. The resistivity, ρ , and Seebeck coefficient, S , for these materials decrease with increased Ga-doping while both mobility and effective mass increase with Ga doping. The power factor (S^2/ρ) therefore increases with Ga-doping however the highest thermoelectric figure of merit ($ZT = 0.39$ at 700 K) was obtained for the composition that had the lowest thermal conductivity. Our results suggest an approach for optimizing the thermoelectric properties of these materials and are part of the continuing effort to explore different quaternary chalcogenide compositions and structure types, as this class of materials continues to be of interest for energy-related applications.

© 2015 Elsevier B.V. All rights reserved.

1. Introduction

The specific material property requirements for good thermoelectric materials can be quantified by the dimensionless figure of merit $ZT = S^2T/\rho\kappa$, where S is the Seebeck coefficient, ρ the electrical resistivity, T the absolute temperature, and κ the total thermal conductivity, $\kappa = \kappa_L + \kappa_E$ (κ_L and κ_E are the lattice and electronic contributions, respectively) [1]. Semiconductors with narrow band gaps are generally considered to be good candidate materials for thermoelectric applications [1,2]. Certain materials with relatively large band gaps, quaternary chalcogenides for example [3,4], have recently been investigated and also shown to possess good thermoelectric properties [5–8].

P-type quaternary chalcogenides have shown good thermoelectric properties mainly due to their relatively low κ in addition to the fact that good electrical properties can be achieved by appropriate modification of their compositions [5–7,9,10]. For example, Fe doping resulted in a lower κ for $\text{Cu}_2\text{ZnGeSe}_4$ [8]. In doping resulted in enhanced electrical conductivity for $\text{Cu}_2\text{ZnSnSe}_4$ [11,12], Cu-excess on the Cd site in $\text{Cu}_{2+x}\text{Cd}_{1-x}\text{SnSe}_4$ [10], on the Zn site in $\text{Cu}_{2+x}\text{Zn}_{1-x}\text{SnSe}_4$ [5] and on the Sn site in $\text{Cu}_{2+x}\text{ZnSn}_{1-x}\text{Se}_4$ [13] resulted in an increase in electrical conductivity as well as a

decrease in κ . In this report we present an investigation of the transport properties of Ga-doped $\text{Cu}_2\text{ZnSnSe}_4$ with and without excess Cu for the first time and describe an approach towards enhanced thermoelectric properties as compared with other kesterite compositions.

2. Experimental

All specimens were prepared by reaction of the high purity elements. The Cu powder (99.9%, Alfa Aesar), Zn shot (99.9999%, Alfa Aesar), Ga pellets (99.9999%, Alfa Aesar), Sn powder (99.999%, Alfa Aesar), and Se powder (99.999%, Alfa Aesar) used for synthesizing the materials in this study were loaded into silica ampoules in the atomic ratios shown in Table 1.¹ The ampoules were sealed in quartz tubes under vacuum (0.1 Pa), heated to 973 K, and subsequently held at this temperature for 5 days before they were air quenched to room temperature. The products were then ground into powders, cold pressed into pellets and annealed at 873 K for one week. The resulting pellets were ground into fine powders (~325 mesh) and loaded into graphite dies for hot pressing.

¹ Certain commercial equipment, instrumentation, or materials are identified in this document. Such identification does not imply recommendation or endorsement by the National Institute of Standards and Technology, nor does it imply that the products identified are necessarily the best available for the purpose.

* Corresponding author.

E-mail address: gnolas@usf.edu (G.S. Nolas).

Table 1
Nominal composition, EDS composition, and room temperature ρ , S , p , μ_H and m^* of all specimens prepared for this study.

Nominal composition	EDS composition	ρ (mOhm-cm)	S ($\mu\text{V/K}$)	p (10^{20} cm^{-3})	μ_H ($\text{cm}^2 \text{ V}^{-1} \text{ s}^{-1}$)	m^* (m_e)
(a) $\text{Cu}_2\text{ZnSnSe}_4$	$\text{Cu}_2\text{Zn}_{0.97}\text{Sn}_{0.97}\text{Se}_{3.96}$	1.0×10^3	353	0.03	1.9	0.5
(b) $\text{Cu}_2\text{ZnGa}_{0.03}\text{Sn}_{0.97}\text{Se}_4$	$\text{Cu}_2\text{Zn}_{1.02}\text{Ga}_{0.02}\text{Sn}_{0.98}\text{Se}_{3.87}$	9.7	146	2.4	2.7	1.7
(c) $\text{Cu}_2\text{ZnGa}_{0.05}\text{Sn}_{0.95}\text{Se}_4$	$\text{Cu}_2\text{Zn}_{1.05}\text{Ga}_{0.05}\text{Sn}_{0.98}\text{Se}_{3.92}$	7.0	122	3.6	2.5	1.8
(d) $\text{Cu}_2\text{ZnGa}_{0.07}\text{Sn}_{0.93}\text{Se}_4$	$\text{Cu}_2\text{Zn}_{1.02}\text{Ga}_{0.06}\text{Sn}_{0.96}\text{Se}_{3.84}$	6.4	113	5.3	1.8	2.1
(e) $\text{Cu}_2\text{ZnGa}_{0.1}\text{Sn}_{0.9}\text{Se}_4$	$\text{Cu}_2\text{Zn}_{1.03}\text{Ga}_{0.09}\text{Sn}_{0.92}\text{Se}_{3.88}$	4.7	103	5.4	2.5	1.9
(f) $\text{Cu}_{2.1}\text{Zn}_{0.9}\text{Ga}_{0.04}\text{Sn}_{0.96}\text{Se}_4$	$\text{Cu}_{2.1}\text{Zn}_{0.94}\text{Ga}_{0.04}\text{Sn}_{0.97}\text{Se}_{3.95}$	1.5	57.2	17	2.4	2.1
(g) $\text{Cu}_{2.2}\text{Zn}_{0.8}\text{Ga}_{0.06}\text{Sn}_{0.94}\text{Se}_4$	$\text{Cu}_{2.2}\text{Zn}_{0.86}\text{Ga}_{0.05}\text{Sn}_{0.96}\text{Se}_{3.94}$	1.3	54.1	18	2.6	2.1
(h) $\text{Cu}_{2.3}\text{Zn}_{0.7}\text{Ga}_{0.12}\text{Sn}_{0.88}\text{Se}_4$	$\text{Cu}_{2.3}\text{Zn}_{0.74}\text{Ga}_{0.09}\text{Sn}_{0.93}\text{Se}_{3.93}$	1.0	45.3	20	3.1	1.9

Densification was accomplished by hot pressing at 673 K and 160 MPa for 3 h under N_2 flow. High density polycrystalline specimens (>96% theoretical density) were obtained after hot pressing, as indicated by measurement of the dimensions and weight of each pressed pellet.

X-ray diffraction (XRD) and energy dispersive spectroscopy (EDX) were used to examine the purity, homogeneity, and chemical composition of the specimens. Powder XRD data were collected with a Bruker D8 Focus diffractometer in Bragg–Brentano geometry using $\text{Cu K}\alpha$ radiation and a graphite monochromator. EDX analyses were accomplished with an Oxford INCA X-Sight 7582M equipped scanning electron microscope (JEOL JSM-6390LV). The homogeneity of the specimens was investigated from twelve EDX data sets obtained from random positions across the dense pellet for each specimen. The EDS data were normalized to the Cu content for each specimen in this study.

The hot pressed pellets were cut using a wire saw into parallelepipeds for transport measurements and Hall measurements. High temperature κ values were determined using the equation $\kappa = D\alpha C_p$, where D is the density, α the thermal diffusivity, and C_p the specific heat. Thermal diffusivity measurements employed the laser flash method in a flowing Ar environment with a NETZSCH LFA 457 system. The uncertainty in the thermal diffusivity measurements was 5%. Heat capacity C_p ($\approx C_v$) was estimated by the Dulong–Petit limit ($C_v = 3nR$, where n is the number of atoms per formula unit and R is the ideal gas constant). At high temperature this may result in an underestimate of C_p thus affecting κ , however, it is a relatively good method for comparing the effect of doping and small compositional changes since it eliminates the uncertainties associated with C_p measurements [14]. High temperature S and ρ were measured with an ULVAC ZEM-3 system (experimental uncertainty of 5%–8% for S and ρ at elevated temperatures). Room temperature Hall measurements were conducted on $0.5 \times 2 \times 5 \text{ mm}^3$ parallelepipeds at multiple positive and negative magnetic fields in order to mitigate voltage probe misalignment effects ($\pm 5\%$ uncertainty).

3. Results and discussion

Fig. 1 shows the indexed powder XRD patterns of the specimens prepared for this study. The XRD data for all specimens can be indexed to the kesterite phase (space group $\bar{I}4$), as has been reported previously by neutron scattering employing a similar materials preparation approach [15] as well as other techniques [16,17].

Fig. 2 shows the temperature dependent ρ (a), S (b) and power factor PF ($=S^2/\rho$) (c) of all specimens investigated in this study. While $\text{Cu}_2\text{ZnSnSe}_4$ exhibits relatively high ρ and S values, as expected for a relatively wide band gap semiconductor [3–5,8], ρ and S of the doped specimens increase with increasing temperature indicating thermally activated semiconductor behavior. The positive sign of S for all specimens implies that holes are the dominant

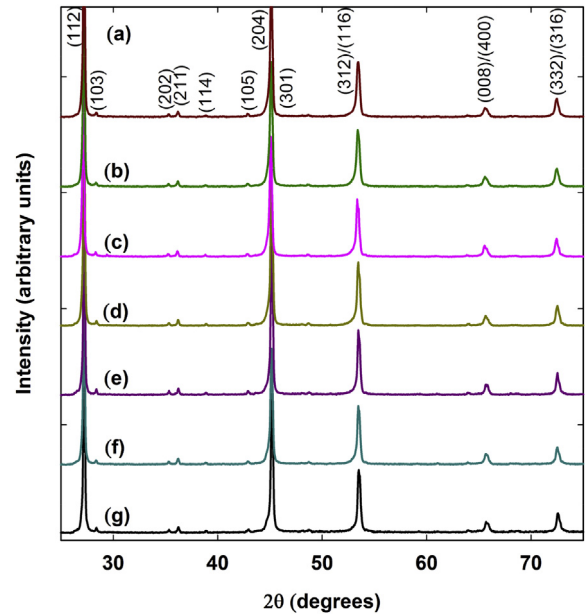


Fig. 1. Indexed powder XRD patterns of (a) $\text{Cu}_2\text{ZnGa}_{0.03}\text{Sn}_{0.97}\text{Se}_4$, (b) $\text{Cu}_2\text{ZnGa}_{0.05}\text{Sn}_{0.95}\text{Se}_4$, (c) $\text{Cu}_2\text{ZnGa}_{0.07}\text{Sn}_{0.93}\text{Se}_4$, (d) $\text{Cu}_2\text{ZnGa}_{0.1}\text{Sn}_{0.9}\text{Se}_4$, (e) $\text{Cu}_{2.1}\text{Zn}_{0.9}\text{Ga}_{0.04}\text{Sn}_{0.96}\text{Se}_4$, (f) $\text{Cu}_{2.2}\text{Zn}_{0.8}\text{Ga}_{0.06}\text{Sn}_{0.94}\text{Se}_4$, and (g) $\text{Cu}_{2.3}\text{Zn}_{0.7}\text{Ga}_{0.12}\text{Sn}_{0.88}\text{Se}_4$.

carriers (p-type conduction), confirmed by Hall measurements (Table 1). The ρ and S values decrease with increasing Ga doping and result in an increase in PF with increasing Ga content. In addition to Ga doping, an excess of Cu further reduced ρ , resulting in a significant increase in PF . The highest PF corresponds to $\text{Cu}_{2.1}\text{Zn}_{0.9}\text{Ga}_{0.04}\text{Sn}_{0.96}\text{Se}_4$ with a carrier density of $1.72 \times 10^{21} \text{ cm}^{-3}$.

Room temperature ρ , S , carrier concentration, p , Hall mobility, μ_H , and effective mass, m^* , for all compositions are listed in Table 1. $\text{Cu}_2\text{ZnSnSe}_4$ has a direct band gap at the Γ point [18], therefore we estimated m^* based on a single parabolic band model where S and p are given by [1]

$$S = \frac{k_B}{e} \left(\frac{(2+r)F_{1+r}(\eta)}{(1+r)F_r(\eta)} - \eta \right) \quad (1)$$

and

$$p = \frac{4\pi(2m_e k_B T)^{3/2}}{h^3} \left(\frac{m^*}{m_e} \right)^{3/2} F_{1/2}(\eta). \quad (2)$$

Here r is the exponent of the energy dependence of the hole mean free path, η ($=E_F k_B^{-1} T^{-1}$ where E_F is the Fermi energy) is the reduced Fermi energy, F_r is the Fermi integral of order r [19,20], m_e is the free electron mass and h is the Planck constant. For scattering from lattice vibrations (acoustic phonons) $r = 0$ and for ionized

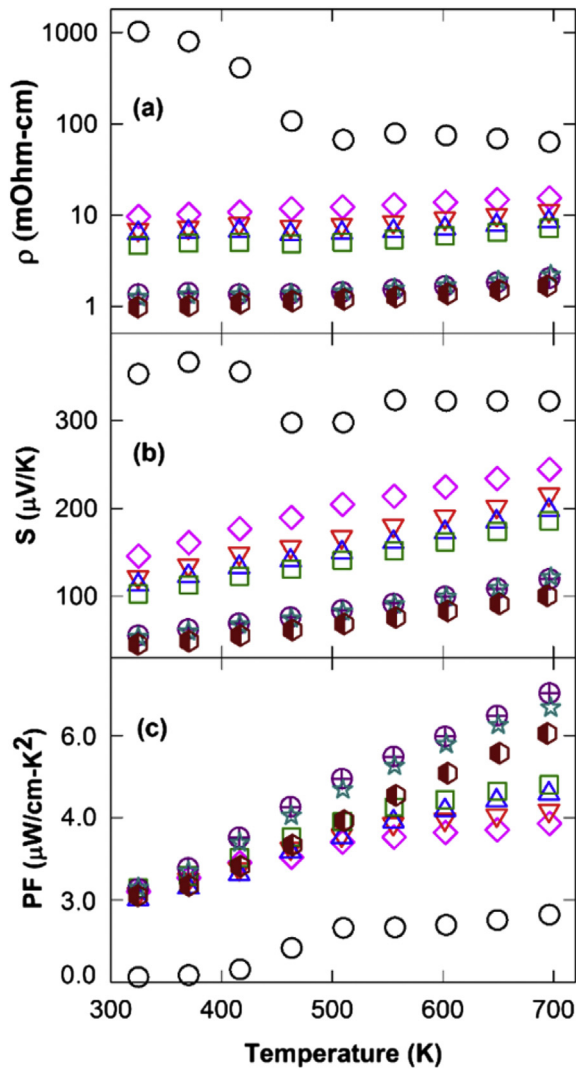


Fig. 2. Temperature dependent (a) ρ (plotted in log-linear scale), (b) S , and (c) PF of $\text{Cu}_2\text{ZnSnSe}_4$ (\circ), $\text{Cu}_2\text{ZnGa}_{0.03}\text{Sn}_{0.97}\text{Se}_4$ (\diamond), $\text{Cu}_2\text{ZnGa}_{0.05}\text{Sn}_{0.95}\text{Se}_4$ (∇), $\text{Cu}_2\text{ZnGa}_{0.07}\text{Sn}_{0.93}\text{Se}_4$ (\triangle), $\text{Cu}_2\text{ZnGa}_{0.1}\text{Sn}_{0.9}\text{Se}_4$ (\square), $\text{Cu}_{2.1}\text{Zn}_{0.9}\text{Ga}_{0.04}\text{Sn}_{0.96}\text{Se}_4$ (\oplus), $\text{Cu}_{2.2}\text{Zn}_{0.8}\text{Ga}_{0.06}\text{Sn}_{0.94}\text{Se}_4$ (\star), and $\text{Cu}_{2.3}\text{Zn}_{0.7}\text{Ga}_{0.12}\text{Sn}_{0.88}\text{Se}_4$ (\bullet).

impurity scattering $r = 2$. Due to the high p values for our doped compositions both lattice vibrations and impurity scattering are assumed thus we used $r = 1$ in our estimates of m^* . As shown in Table 1, with both Ga-doping and excess Cu μ_H increased from $1.9 \text{ cm}^2 \text{ V}^{-1} \text{ S}^{-1}$ to $3.1 \text{ cm}^2 \text{ V}^{-1} \text{ S}^{-1}$ and m^* increased from $0.5 m_e$ to $2.1 m_e$. Our μ_H values are comparable to that for In-doping [11,12] while m^* are much larger, with the highest PF among all specimens shown in Table 1 being that with the largest m^* .

Fig. 3 shows the temperature dependent κ (a) and ZT (b) of the specimens prepared for this study. The κ values decrease with increasing temperature without an “upturn” at higher temperatures, indicative of little or no bipolar contribution to κ in the measured temperature range for all specimens. Due to higher charge densities the κ values increase with increased Ga-doping in the Cu-excess compositions; κ_E increasing substantially with decreasing ρ . Although an excess in Cu results in enhanced thermoelectric properties for $\text{Cu}_2\text{ZnSnSe}_4$ [5,13], our investigation indicates that this is not the case here. $\text{Cu}_2\text{ZnGa}_{0.05}\text{Sn}_{0.95}\text{Se}_4$ resulted in the highest ZT (0.39 at 700 K) among all specimens, as compared with $ZT = 0.25$ at 700 K for In-doping [11].

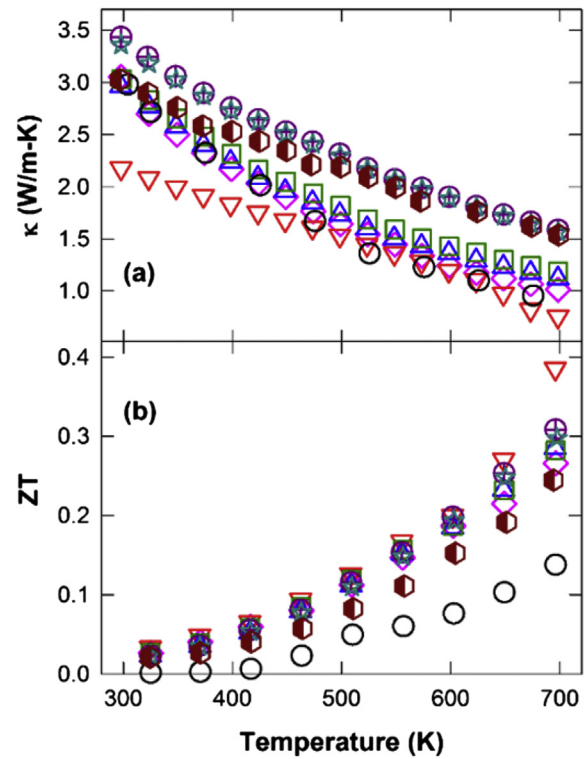


Fig. 3. Temperature dependent (a) κ and (b) ZT of all specimens. The symbols corresponding to each specimen are as defined in Fig. 2.

4. Conclusions

We have investigated Ga-doping with and without excess Cu in $\text{Cu}_2\text{ZnSnSe}_4$ in order to investigate the high temperature transport properties of kesterite quaternary chalcogenides. The μ_H and m^* values increase from $1.9 \text{ cm}^2 \text{ V}^{-1} \text{ S}^{-1}$ to $3.1 \text{ cm}^2 \text{ V}^{-1} \text{ S}^{-1}$ and $0.5 m_e$ to $2.1 m_e$, respectively, as a result of Ga-doping with excess Cu, with the PF increasing from $1.64 \text{ } \mu\text{W}/\text{cm-K}^2$ to $7.03 \text{ } \mu\text{W}/\text{cm-K}^2$ at 700 K. A ZT value of 0.39 was obtained for $\text{Cu}_2\text{ZnGa}_{0.05}\text{Sn}_{0.95}\text{Se}_4$ at 700 K, with higher ZT values expected at higher temperatures. Our investigation may also indicate that Cu-excess on the Zn site is less effective in improving ZT in kesterite compositions as compared with that of stannite compositions.

Acknowledgments

This work was supported, in part, by the National Science Foundation Grant No. DMR-1400957. K.W. acknowledges support from the II-VI Foundation Block-Gift Program. H.W. and W.D.P. would like to thank the support of the assistant secretary for Energy Efficiency and Renewable Energy of the Department of Energy and the Propulsion Materials program under the Vehicle Technologies program. Oak Ridge National Laboratory is managed by UT-Battelle LLC under contract DE-AC05000OR22725.

References

- [1] G.S. Nolas, J.W. Sharp, H.J. Goldsmid, *Thermoelectrics: Basics Principles and New Materials Developments*, Springer-Verlag, Berlin, Germany, 2001.
- [2] G.D. Mahan, Figure of merit for thermoelectrics, *J. Appl. Phys.* 65 (1989) 1578–1583.
- [3] H. Matsushita, T. Ichikawa, A. Katsui, Structural, thermodynamical and optical properties of $\text{Cu}_2\text{-II-IV-VI}_4$ quaternary compounds, *J. Mater. Sci.* 40 (2005) 2003–2005.
- [4] J.L. Shay, J.H. Wernick, B.R. Pamplin, *Ternary Chalcopyrite Semiconductors*:

- Growth, Electronic Properties, and Applications, Pergamon, Great Britain, 1975.
- [5] Y. Dong, H. Wang, G.S. Nolas, Synthesis and thermoelectric properties of Cu excess $\text{Cu}_2\text{ZnSnSe}_4$, *Phys. Status Solidi RRL* 8 (2014) 61–64.
- [6] Y. Dong, H. Wang, G.S. Nolas, Synthesis, crystal structure, and high temperature transport properties of p-Type $\text{Cu}_2\text{Zn}_{1-x}\text{Fe}_x\text{SnSe}_4$, *Inorg. Chem.* 52 (2013) 14364–14367.
- [7] M. Ibanez, R. Zamani, A. LaLonde, D. Cadavid, W. Li, A. Shavel, J. Arbiol, J.R. Morante, S. Gorsse, G.J. Snyder, A. Cabot, $\text{Cu}_2\text{ZnGeSe}_4$ nanocrystals: synthesis and thermoelectric properties, *J. Am. Chem. Soc.* 134 (2012) 4060–4063.
- [8] W.G. Zeier, Y. Pei, G. Pomrehn, T. Day, N. Heinz, C.P. Heinrich, G.J. Snyder, W. Tremel, Phonon scattering through a local anisotropic structural disorder in the thermoelectric solid solution $\text{Cu}_2\text{Zn}_{1-x}\text{Fe}_x\text{GeSe}_4$, *J. Am. Chem. Soc.* 135 (2013) 726–732.
- [9] M.-L. Liu, F.-Q. Huang, L.-D. Chen, I.-W. Chen, A wide-band-gap p-type thermoelectric material based on quaternary chalcogenides of $\text{Cu}_2\text{ZnSnQ}_4$ ($Q = \text{S}, \text{Se}$), *Appl. Phys. Lett.* 94 (2009), 202103/1–202103/3.
- [10] M. Ibanez, D. Cadavid, R. Zamani, N. Garcia-Costello, V. Izquierdo-Roca, W. Li, A. Fairbrother, J.D. Prades, A. Shavel, J. Arbiol, A. Perez-Rodriguez, J.R. Morante, A. Cabot, Composition control and thermoelectric properties of quaternary chalcogenide nanocrystals: the case of stannite $\text{Cu}_2\text{CdSnSe}_4$, *Chem. Mater.* 24 (2012) 562–570.
- [11] R. Chetty, M. Falmbigl, P. Rogl, P. Heinrich, E. Royanian, E. Bauer, S. Suwas, R.C. Mallik, The effect of multisubstitution on the thermoelectric properties of chalcogenide-based $\text{Cu}_{2-x}\text{Zn}_{0.9}\text{Sn}_{1-x}\text{In}_x\text{Se}_4$ ($0 \leq x \leq 0.1$), *Phys. Status Solidi A* 210 (2013) 2471–2478.
- [12] D.-H. Kuo, M. Tsega, Electrical conduction and mobility enhancement in p-type in-doped $\text{Cu}_2\text{ZnSnSe}_4$ bulks, *Jpn. J. Appl. Phys.* 53 (2014), 035801/1–035801/4.
- [13] Ch Raju, M. Falmbigl, P. Rogl, X. Yan, E. Bauer, J. Horky, M. Zehetbauer, R.C. Mallik, Thermoelectric properties of chalcogenide based $\text{Cu}_{2+x}\text{ZnSn}_{1-x}\text{Se}_4$, *AIP Adv.* 3 (2013), 032106/1–032106/12.
- [14] H. Wang, W.D. Porter, H. Bottner, J. Kronig, L. Chen, S. Bai, T.M. Tritt, A. Mayolet, J. Senawiratne, C. Smith, F. Harris, P. Gilbert, J. Sharp, J. Lo, H. Kleinke, L. Kiss, Transport properties of bulk thermoelectrics: an international round-robin study, part II: thermal diffusivity, specific heat, and thermal conductivity, *J. Electron. Mater.* 42 (2013) 1073–1084.
- [15] S. Schorr, The crystal structure of kesterite type compounds: a neutron and X-ray diffraction study, *Sol. Energy Mater. Sol. Cells* 95 (2011) 1482–1488.
- [16] D. Kuciauskas, I. Repins, A. Kanevce, J.V. Li, P. Dippo, C.L. Beall, Time-resolved recombination analysis in kesterite polycrystalline thin films and photovoltaic devices with one-photon and two-photon excitation, *Sol. Energy Mater. Sol. Cells* 136 (2015) 100–105.
- [17] P. Kush, S. Deka, Photoelectrical properties of surfactant-free kesterite $\text{Cu}_2\text{ZnSnSe}_4$ hydrophilic nanocrystal ink and the stability in polar solvents, *J. Nanopart. Res.* 16 (2014), 2600/1–2600/14.
- [18] S. Nakamura, T. Maeda, T. Tabata, T. Wada, First-principles study of indium-free photovoltaic compounds $\text{Ag}_2\text{ZnSnSe}_4$ and $\text{Cu}_2\text{ZnSnSe}_4$, in: *Proceeding of the 37th IEEE Photovoltaic Specialist Conference*, Washington State Convention Center, Seattle, Washington, USA, 2011, pp. 785–786.
- [19] P. Rhodes, Fermi–Dirac functions of integral order, *Proc. R. Soc. Lond. A* 204 (1950) 396–405.
- [20] J. McDougall, E.C. Stoner, The computation of Fermi–Dirac functions, *Philos. Trans. R. Soc. Lond. A* 237 (1938) 67–104.